New Journal of Physics
The open access journal at the forefront of physics

Deutsche Physikalische Gesellschaft DPG IOP Institute of Physics

PAPER • OPEN ACCESS

Maximum power and corresponding efficiency for two-level heat engines and refrigerators: optimality of fast cycles

To cite this article: P A Erdman *et al* 2019 *New J. Phys.* **21** 103049

IOP Publishing New J. Phys. 21 (2019) 103049 https://doi.org/10.1088/1367-2630/ab4dca

New Journal of Physics
The open access journal at the forefront of physics

Deutsche Physikalische Gesellschaft DPG
IOP Institute of Physics

Published in partnership with: Deutsche Physikalische Gesellschaft and the Institute of Physics

CrossMark

OPEN ACCESS

RECEIVED
20 June 2019

REVISED
3 October 2019

ACCEPTED FOR PUBLICATION
15 October 2019

PUBLISHED
29 October 2019

PAPER

Maximum power and corresponding efficiency for two-level heat engines and refrigerators: optimality of fast cycles

P A Erdman[1], **V Cavina**[1], **R Fazio**[1,2], **F Taddei**[3] **and V Giovannetti**[1]

[1] NEST, Scuola Normale Superiore and Istituto Nanoscienze-CNR, I-56126 Pisa, Italy
[2] ICTP, Strada Costiera 11, I-34151 Trieste, Italy
[3] NEST, Istituto Nanoscienze-CNR and Scuola Normale Superiore, I-56126 Pisa, Italy

E-mail: paolo.erdman@sns.it

Keywords: quantum thermodynamics, quantum heat engine, maximum power, efficiency at maximum power, optimal control

Abstract

We study how to achieve the ultimate power in the simplest, yet non-trivial, model of a thermal machine, namely a two-level quantum system coupled to two thermal baths. Without making any prior assumption on the protocol, via optimal control we show that, regardless of the microscopic details and of the operating mode of the thermal machine, the maximum power is universally achieved by a fast Otto-cycle like structure in which the controls are rapidly switched between two extremal values. A closed formula for the maximum power is derived, and finite-speed effects are discussed. We also analyze the associated efficiency at maximum power showing that, contrary to universal results derived in the slow-driving regime, it can approach Carnot's efficiency, no other universal bounds being allowed.

1. Introduction

Two thermal baths in contact through a working fluid that can be externally driven represent the prototypical setup that has been studied from the origin of thermodynamics up to our days. The energy balance can be described in terms of three quantities: the work extracted from the fluid and the heat exchanged with the hot/cold baths. The fundamental limitations to the inter-conversion of heat into work stem from the concept of irreversibility and are at the core of the second law of thermodynamics. A working medium in contact with two baths at different temperatures is also significant from a practical point of view, since it is the paradigm behind the following specific machines: the heat engine, the refrigerator [1–4], the thermal accelerator [5], and the heater [5].

Quantum thermodynamics [6–8] has emerged both as a field of fundamental interest, and as a potential candidate to improve the performance of thermal machines [9–23]. The optimal performance of these systems has been discussed within several frameworks and operational assumptions, ranging from low-dissipation and slow driving regimes[24–28], to shortcuts to adiabaticity approaches [29–32], to endoreversible engines [33, 34]. Several techniques have been developed for the optimal control of two-level systems for achieving a variety of goals: from optimizing the speed [35–37], to generating efficient quantum gates [38, 39], to controlling dissipation [40, 41], and to optimizing thermodynamic performances [42–47].

The aim of the present paper is to find the optimal strategy to deliver maximum power in all four previously mentioned machines. We perform this optimization in the simplest, yet non-trivial, model of a machine which, in the spirit of quantum thermodynamics, is based on a two-level quantum system as working fluid. As opposed to current literature, we explicitly carry out the power maximization without making any assumptions on the operational regime, nor on the speed of the control parameters, nor on the specific coupling between the working fluid and the bath. We find that, if the evolution of the working medium is governed by a Markovian master equation (MME) [48, 49], the optimal driving takes a universal form: an infinitesimal Otto-cycle-like structure in which the control parameters must be varied between two extremal values as fast as possible. This is our first main results, described in equation (8). Surprisingly, the optimal solution is achieved in the

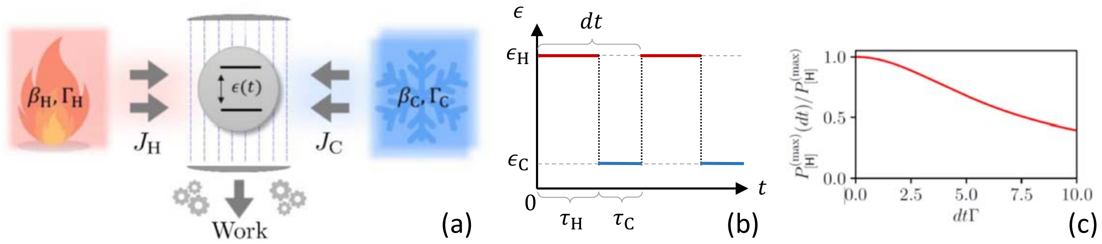

Figure 1. (a) Schematic representation of the setup. S (gray circle) is externally driven by modulating the level spacing $\epsilon(t)$ and coupled with the hot bath H (red box) and the cold bath C (blue box) at inverse temperatures β_H and β_C. J_H and J_C are the heat currents leaving the baths, while Γ_H and Γ_C are the associated dissipation rates. Depending on the controls the system can operates either as an heat engine (mode [E]), as a refrigerator (mode [R]), as a thermal accelerator (mode [A]), or as a heater (mode [H]). (b) Representation of the optimal protocol that maximizes the power in the limit $dt \to 0$; and (c) power in mode [H] for finite values of $dt\Gamma$ normalized to the maximum power. We assume a single bath coupled to S characterized by a dissipation rate $\Gamma(\epsilon)$ such that $\Gamma(\epsilon) = \Gamma(-\epsilon)$. In this case, the maximization in equation (8) yields $\epsilon_H^* = -\epsilon_C^*$, and Γ in (c) denotes $\Gamma(\epsilon_H^*)$.

'fast-driving' regime, i.e. when the driving frequency is faster than the typical dissipation rate induced by the baths, which has received little attention in literature [50–52].

By applying our optimal protocol to heat engines and refrigerators, we find new theoretical bounds on the efficiency at maximum power (EMP). Many upper limits to the EMP, strictly smaller than Carnot's efficiency, have been derived in literature, such as the Curzon–Ahlborn and Schmiedl–Seifert efficiencies. The Curzon–Ahlborn efficiency emerges in various specific models [53–55], and it has been derived by general arguments from linear irreversible thermodynamics [56]. The Schmiedl–Seifert efficiency has been proven to be universal in cyclic Brownian heat engines [57] and for any driven system operating in the slow-driving regime [24]. By studying the efficiency of our system at the ultimate power, i.e. in the fast-driving regime, we prove that there is no fundamental upper bound to the EMP. Indeed, we show that the Carnot efficiency is reachable *at maximum power* through a suitable engineering of the bath couplings. This is our second main results, illustrated in figures 2(b), (c) and figure 3. In view of experimental implementations, we assess the impact of finite-time effects on our optimal protocol, finding that the maximum power does not decrease much if the external driving is not much slower than the typical dissipation rate induced by the baths [58, 59]. Furthermore, we apply our optimal protocol to two experimentally accessible models, namely photonic baths coupled to a qubit [22, 60–63] and electronic leads coupled to a quantum dot [21, 23, 58, 59, 64, 65].

2. Maximum power

The setup we consider consists of a two-level quantum system S with energy gap $\epsilon(t)$ that can be externally modulated[4]. As schematically shown in figure 1(a), the system is placed in thermal contact with two reservoirs, the hot bath H at inverse temperature β_H and the cold bath C at inverse temperature β_C, respectively characterized by coupling constants $\lambda_H(t)$ and $\lambda_C(t)$ that can be modulated in time. The system can operate in four different modes: (i) the heat engine mode [E], where S is used to produce work by extracting heat from H while donating it to C; (ii) the refrigerator mode [R], where S is used to extract heat from C; (iii) the thermal accelerator mode [A], where S operates to move as much heat as possible to C; (iv) the heater mode [H], where we simply use S to deliver as much heat as possible to both H and C. Assuming cyclic modulation of the controls (i.e. of $\epsilon(t)$, $\lambda_H(t)$ and $\lambda_C(t)$) we are interested in maximizing the corresponding averaged output powers of each operating mode, i.e. the quantities

$$P_{[E]} = \langle J_H \rangle + \langle J_C \rangle, \qquad P_{[R]} = \langle J_C \rangle, \tag{1}$$

$$P_{[A]} = -\langle J_C \rangle, \qquad P_{[H]} = -\langle J_H \rangle - \langle J_C \rangle, \tag{2}$$

where J_H and J_C are the instantaneous heat fluxes entering the hot and cold reservoirs respectively, and where the symbol $\langle \cdots \rangle$ stands for temporal average over a modulation cycle of the controls. To tackle the problem we adopt a MME approach [60], namely we write

$$\frac{d}{dt}\hat{\rho} = -\frac{i}{\hbar}[\hat{H}, \hat{\rho}]_- + \sum_{\alpha=H,C} D_\alpha[\hat{\rho}], \tag{3}$$

[4] In principle, one can consider a broader family of controls including the possibility of rotating the Hamiltonian eigenvectors; however there is evidence that such an additional freedom does not help in two-level systems [45, 46].

where $\hat{\rho}$ is the density matrix of the two-level system at time t, $\hat{\mathcal{H}} := \epsilon(t)\hat{\sigma}_+\hat{\sigma}_-$ its local Hamiltonian, and

$$\mathcal{D}_\alpha[\cdots] := \sum_{i=\pm} \lambda_\alpha(t)\Gamma_\alpha^{(i)}(\epsilon(t))(\hat{\sigma}_i \cdots \hat{\sigma}_i^\dagger - \frac{1}{2}[\hat{\sigma}_i^\dagger\hat{\sigma}_i, \cdots]_+) \tag{4}$$

is the Gorini–Kossakowski–Sudarshan–Lindblad dissipator [48, 49] associated with the bath $\alpha = \mathrm{H, C}$. We have denoted with $\hat{\sigma}_+$ and $\hat{\sigma}_-$ the raising and lowering operators of S and with the symbol $[\cdots,\cdots]_\mp$ the commutator $(-)$ and anti-commutator $(+)$ operations. $\mathcal{D}_\alpha$ is characterized by dissipation rates $\Gamma_\alpha^{(i=\pm)}(\epsilon)$ and by the dimensionless coupling constant $\lambda_\alpha(t) \in [0, 1]$ that plays the role of a 'switch' control parameter. It is worth noticing that, since $[\hat{\mathcal{H}}(t), \hat{\mathcal{H}}(t')] = 0$, the MME we employ is valid also in the fast-driving regime, provided that the correlation time of the bath is the smallest timescale in our problem [66]. Therefore, the fast-driving regime is characterized by a control frequency which is faster than the typical dissipation rate, but slower than the inverse correlation time of the bath. Furthermore, we assume that the Hamiltonain $\hat{\mathcal{H}}_{\mathrm{int}}$, describing the system-bath interaction, is such that its expectation value on the Gibbs state of the baths is zero (this is true, for example, for tunnel-like Hamiltonians, where the number of creation/annihilation operators of the bath entering $\hat{\mathcal{H}}_{\mathrm{int}}$ is odd). Such assumption guarantees that no work is necessary to switch on and off the coupling between the system and the baths.

Without assigning any specific value to the dissipation rates, we only require them to obey the detailed balance equation $\Gamma_\alpha^{(+)}(\epsilon)/\Gamma_\alpha^{(-)}(\epsilon) = \mathrm{e}^{-\beta_\alpha\epsilon}$. This ensures that, at constant level spacing ϵ, the system S will evolve into a thermal Gibbs state characterized by an excitation probability

$$p_{\mathrm{eq}}^{(\alpha)}(\epsilon) := \frac{\Gamma_\alpha^{(+)}(\epsilon)}{\Gamma_\alpha^{(+)}(\epsilon) + \Gamma_\alpha^{(-)}(\epsilon)} = \frac{1}{1 + \mathrm{e}^{\beta_\alpha\epsilon}} \tag{5}$$

when in contact only with heat bath α. For simplicity, we consider the system to be coupled to one heat bath at the time, i.e. we assume that $\lambda_{\mathrm{H}}(t) + \lambda_{\mathrm{C}}(t) = 1$, and that $\lambda_\alpha(t)$ can take the values 0 or 1. As we shall see in the following, this constraint, as well as the possibility of controlling the coupling constants $\lambda_\alpha(t)$, is not fundamental to derive our results, at least for those cases where the effective dissipation rate

$$\Gamma_\alpha(\epsilon) := \Gamma_\alpha^{(+)}(\epsilon) + \Gamma_\alpha^{(-)}(\epsilon) \tag{6}$$

of each bath is sufficiently peaked around distinct values. The instantaneous heat flux leaving the thermal bath α can now be expressed as [62]

$$J_\alpha = \mathrm{tr}[\hat{\mathcal{H}}\mathcal{D}_\alpha[\hat{\rho}]] = -\epsilon(t)\lambda_\alpha(t)\Gamma_\alpha[\epsilon(t)](p(t) - p_{\mathrm{eq}}^{(\alpha)}[\epsilon(t)]),$$

where $p(t) := \mathrm{tr}[\hat{\sigma}_+\hat{\sigma}_-\hat{\rho}(t)]$ is the probability of finding S in the excited state of $\mathcal{H}$ at time t which obeys the following differential equation

$$\frac{\mathrm{d}}{\mathrm{d}t}p(t) = -\sum_{\alpha=\mathrm{H,C}} \lambda_\alpha(t)\Gamma_\alpha[\epsilon(t)](p(t) - p_{\mathrm{eq}}^{(\alpha)}[\epsilon(t)]), \tag{7}$$

according to the MME specified above. By explicit integration of (7) we can hence transform all the terms in equation (2) into functionals of the controls which can then be optimized with respect to all possible choices of the latter.

As shown in appendix A, we find that the protocols which maximize the average power of a fixed physical setup, i.e. at fixed dissipation rates, are cycles performed in the fast-driving regime, i.e. when the driving frequency is faster than the typical dissipation rate. More precisely, the optimal cycle is such that $\epsilon(t)$ instantaneously jumps between two values ϵ_{H} and ϵ_{C}, see figure 1(b), while being in contact, respectively, only with the hot and cold bath for infinitesimal times τ_{H} and τ_{C} fulfilling the condition $\tau_{\mathrm{H}}/\tau_{\mathrm{C}} = \sqrt{\Gamma_{\mathrm{C}}(\epsilon_{\mathrm{C}})/\Gamma_{\mathrm{H}}(\epsilon_{\mathrm{H}})}$ [5]. As in Otto cycles considered in literature (see the extensive literature on this topic, e.g. [10, 12, 20, 67–69]), no heat is transferred during the jumps and no work is done while the system is in contact with the baths. The resulting maximum power averaged over one period can then be cast into the following compact expression (see appendix B for details)

$$P_{[\nu]}^{(\max)} = \max_{(\epsilon_{\mathrm{H}},\epsilon_{\mathrm{C}})\in\mathcal{C}} \frac{\Gamma_{\mathrm{H}}(\epsilon_{\mathrm{H}})\Gamma_{\mathrm{C}}(\epsilon_{\mathrm{C}})(p_{\mathrm{eq}}^{(\mathrm{H})}(\epsilon_{\mathrm{H}}) - p_{\mathrm{eq}}^{(\mathrm{C})}(\epsilon_{\mathrm{C}})}{(\sqrt{\Gamma_{\mathrm{H}}(\epsilon_{\mathrm{H}})} + \sqrt{\Gamma_{\mathrm{C}}(\epsilon_{\mathrm{C}})})^2} \tilde{\epsilon}_{[\nu]}, \tag{8}$$

where $\nu = \mathrm{E, R, A, H}$ and the quantity $\tilde{\epsilon}_{[\nu]}$ is given by $\tilde{\epsilon}_{[\mathrm{E}]} = \epsilon_{\mathrm{H}} - \epsilon_{\mathrm{C}}$, $\tilde{\epsilon}_{[\mathrm{R}]} = -\epsilon_{\mathrm{C}}$, $\tilde{\epsilon}_{[\mathrm{A}]} = \epsilon_{\mathrm{C}}$, and $\tilde{\epsilon}_{[\mathrm{H}]} = \epsilon_{\mathrm{C}} - \epsilon_{\mathrm{H}}$. In equation (8) $\mathcal{C}$ is the range over which the energy gap $\epsilon(t)$ of S is allowed to be varied according to the possible technical limitations associated with the specific implementation of the setup. Equation (8), which stems from the optimality of the fast-driving regime, is the first main result of the present work. We emphasize that, as opposed to current literature, our closed expression for the maximum power holds for *any* dissipation rate function $\Gamma_{\mathrm{H/C}}(\epsilon)$. In the following we will apply our result to specific implementations

[5] This particular scaling has been found also in the optimization of endoreversible Carnot Heat engines [9].

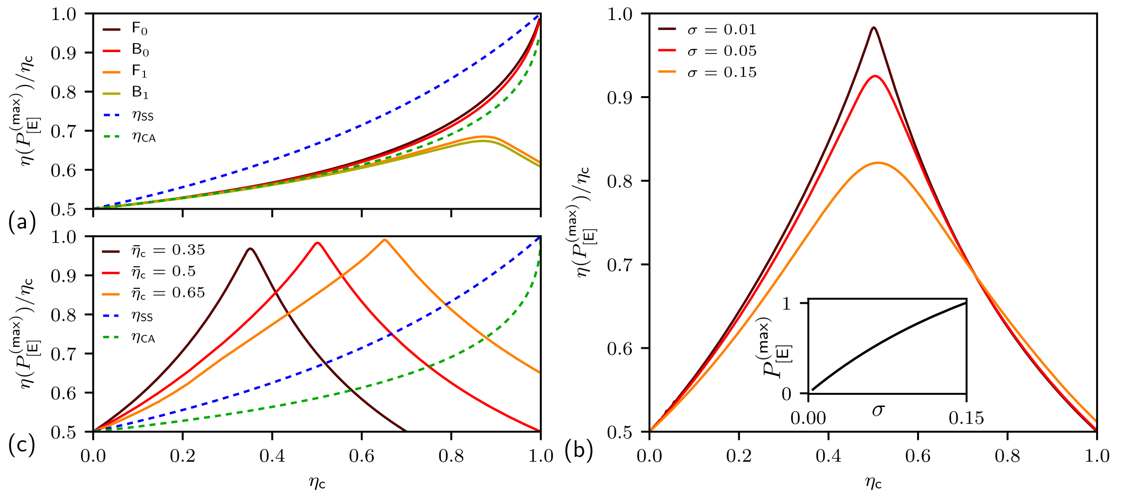

Figure 2. EMP for the heat engine mode [$\eta(P_{[E]}^{(\max)})$ of equation (10)], normalized to η_c, as a function of η_c (varied by fixing β_H and sweeping over β_C). (a) shows $\eta(P_{[E]}^{(\max)})$ for the fermionic models (F_0 and F_1) and the bosonic models (B_0 and B_1) of equation (9) together with the upper bounds η_{SS} [57] and η_{CA} [53]. Notice that as $\eta_c \to 0$ (small baths temperature difference), we have $\eta(P_{[E]}^{(\max)}) \simeq \eta_c/2 + \eta_c^2/8$ as expected. For $\eta_c \to 1$, instead, the value of $\eta(P_{[E]}^{(max)})$ for the models F_1 and B_1 saturates to a finite fraction of η_c, while the F_0 and B_0 models reach Carnot efficiency. The Fermionic model displays a slightly larger $\eta(P_{[E]}^{(\max)})$ than the corresponding bosonic model. In all models we consider symmetric leads, i.e. $k_H = k_C$. Note that $\eta(P_{[E]}^{(\max)})$ does not depend on the value of k_α. (b) and (c) show $\eta(P_{[E]}^{(\max)})$ computed using Lorentzian filtering rates $\Gamma_\alpha(\epsilon_\alpha) = \gamma\sigma^2/(\sigma^2 + (\epsilon_\alpha - \bar{\epsilon}_\alpha)^2)$ with γ, σ and $\bar{\epsilon}_\alpha$ positive constants (systems with multiple quantum-dots in series [73] e.g. exhibit such dependence). In both panels we fix $\bar{\epsilon}_C = 1$. (b): we set $\bar{\epsilon}_H = 2\bar{\epsilon}_C$ such that we expect to approach η_c at $\bar{\eta}_c = 1/2$. Indeed, as σ decreases, $\eta(P_{[E]}^{(\max)})/\eta_c$ approaches one at $\bar{\eta}_c = 1/2$. Conversely, the corresponding maximum power decreases: in the inset, where $P_{[E]}^{(\max)}$ is plotted as a function of σ for $\bar{\eta}_c = 1/2$, we see that the maximum power becomes vanishingly small for $\sigma \to 0$. The power is normalized to the its value for $\sigma = 0.15$, where $P_{[E]}^{(\max)} = 0.0044\gamma\beta_H^{-1}$. (c): At fixed $\sigma = 0.01$, we show that the EMP can approach η_c at any bath temperature. We choose $\bar{\epsilon}_H/\bar{\epsilon}_C = 1/0.65, 1/0.5$ and $1/0.35$, corresponding to $\bar{\eta}_c = 0.35, 0.5$ and 0.65. Energies are expressed in units of $1/\beta_H$, and the EMP does not depend on γ.

which are relevant experimentally and compute their associated efficiencies at maximum power. In particular we shall consider the case of fermionic (F_n) and bosonic (B_n) baths with associated effective rates of the form

$$\Gamma_\alpha^{(F_n)}(\epsilon) = k_\alpha \epsilon^n, \ \Gamma_\alpha^{(B_n)}(\epsilon) = k_\alpha \epsilon^n \coth(\beta_\alpha \epsilon/2), \tag{9}$$

with $n \geqslant 0$ integer and with k_α being a coupling strength constant. The fermionic rate (the first of equation (9)) for instance can describe two electronic leads, with density of states depending on n, tunnel coupled to a single-level quantum-dot [64, 70, 71]; the bosonic one instead is applied in the study of two-level atoms in a dispersive quantum electromagnetic cavity [72].

3. Heat engine mode [E]

It is common belief that the efficiency of a heat engine (work extracted over heat absorbed from the hot bath H), driven at maximum power (EMP), should exhibit a finite gap with respect to the Carnot efficiency $\eta_c := 1 - \beta_H/\beta_C$. Indeed, this is corroborated by various results on EMP bounds: the Curzon–Ahlborn EMP $\eta_{CA} := 1 - \sqrt{1 - \eta_c}$ emerges in various specific models [27, 53, 57], and it has been derived by general arguments from linear irreversible thermodynamics [56], while the Schmiedl–Seifert EMP $\eta_{SS} := \eta_c/(2 - \eta_c)$ has been proven to be universal for any driven system operating in the slow-driving regime [24]. However, the completely out-of-equilibrium and optimal cycles associated with the values of $P_{[E]}^{(\max)}$ reported in equation (8), do not fulfill such assumptions. As a matter of fact, by choosing particular 'energy filtering' dissipation rates $\Gamma_\alpha(\epsilon)$ (instead of the regular ones given e.g. in equation (9)), we can produce configurations which approach Carnot's efficiency with arbitrary precision while delivering maximum power, proving the lack of any fundamental bound to the EMP. Before discussing this highly not trivial effect, it is worth analyzing the performances associated with the baths models of equation (9).

We remind that the efficiency of an Otto cycle heat engine working between the internal energies ϵ_C and ϵ_H is given by $\eta = 1 - \epsilon_C/\epsilon_H$. Accordingly, indicating with ϵ_H^* and ϵ_C^* the values of the gaps that lead to the maximum of the rhs term of equation (8), we write the EMP of our scheme as

$$\eta(P_{[E]}^{(\max)}) = 1 - \epsilon_C^*/\epsilon_H^* = 1 - (1 - \eta_c)\epsilon_C^*\beta_C/\epsilon_H^*\beta_H. \tag{10}$$

In figure 2(a) we report the value of $\eta(P_{[E]}^{(\max)})$ obtained from (10) for the rates of equation (9) for $n = 0, 1$. By a direct comparison with η_{CA} and η_{SS}, one notices that while the second is always respected by our optimal protocol, the first is outperformed at least for the baths F_0 and B_0, confirming the findings of [45, 65, 71]. For small temperature differences between the baths, the EMP can be expanded as a power series in η_c of the form $a_1\eta_c + a_2\eta_c^2 + \cdots$. It has been shown that $a_1 = 1/2$ is a universal property of low dissipation heat engines [24] and, in this context, $a_2 = 1/8$ is associated with symmetric dissipation coefficients. As explicitly discussed in appendix C, we find that also our protocol delivers an EMP with a first order expansion term $a_1 = 1/2$ and with a second order correction $a_2 = 1/8$ achieved if we assume that the two leads are symmetric, i.e. $\Gamma_H(\epsilon, \beta) = \Gamma_C(\epsilon, \beta)$, or if the rates are constants.

We now turn to the possibility of having $\eta(P_{[E]}^{(\max)})$ arbitrarily close to η_c. By a close inspection of the second identity of equation (10) we notice that one can have $\eta(P_{[E]}^{(\max)}) \simeq \eta_c$ for all those models where the maximum power (see equation (8)) is obtained for values of the gaps fulfilling the condition $\epsilon_C^*\beta_C \approx \epsilon_H^*\beta_H$. Consider hence a scenario where the rates $\Gamma_\alpha(\epsilon_\alpha)$ are such that the power is vanishingly small for all values of ϵ_α except for a windows of width σ around a given value $\bar{\epsilon}_\alpha$, a configuration that can be used to eliminate the presence of the activation controls $\lambda_\alpha(t)$ from the problem. Under the assumption of small enough σ, we expect the maximization in equation (8) to yield $\beta_C\epsilon_C^* \approx \beta_H\epsilon_H^*$ when the inverse temperature ratio is $\beta_C/\beta_H \approx \bar{\epsilon}_H/\bar{\epsilon}_C$, so that $\eta(P_{[E]}^{(\max)}) \approx \eta_c$. This is indeed evident from figures 2(b) and (c), where we report the value $\eta(P_{[E]}^{(\max)})$ as a function of η_c (which represents the temperature of the baths) for rates having a Lorentzian shape dependence: by decreasing σ, the EMP approaches Carnot's efficiency at $\bar{\eta}_c := 1 - \bar{\epsilon}_C/\bar{\epsilon}_H = 1/2$ (figure 2(b)), while by tuning the position of the peak of the Lorentzian rates, the EMP can approach Carnot's efficiency at any given bath temperature configuration $\bar{\eta}_c$ (figure 2(c)). We emphasize that even our system with Lorentzian shaped rates would exhibit an EMP bounded by η_{SS} if operated in the slow-driving regime. The possibility of reaching Carnot's EMP is thus a characteristic which emerges thanks to the fast-driving regime. Conversely, as σ decreases and $\eta(P_{[E]}^{(\max)}) \to \eta_c$, the corresponding maximum power tends to zero (see the inset of figure 2(b) where the maximum power, at $\bar{\eta}_c = 1/2$, is plotted as a function of σ).

4. Refrigerator mode [R]

The efficiency of a refrigerator is quantified by the coefficient of performance (COP), i.e. the ratio between the heat extracted from the cold bath and the work done on the system. For an Otto-cylce the COP is given by $C_{op} = \epsilon_C/(\epsilon_H - \epsilon_C)$ which, by replacing the values ϵ_C^*, ϵ_H^* that lead to the maximum $P_{[R]}^{(\max)}$ of equation (8), yields an associated COP at maximum power (CMP) equal to

$$C_{op}(P_{[R]}^{\max}) = \frac{\epsilon_C^*}{(\epsilon_H^* - \epsilon_C^*)} = \left[\frac{\beta_H\epsilon_H^*}{\beta_C\epsilon_C^*}(1/C_{op}^{(c)} + 1) - 1\right]^{-1}, \tag{11}$$

where $C_{op}^{(c)} := \beta_C^{-1}/(\beta_H^{-1} - \beta_C^{-1})$ is the maximum COP dictated by the second law. Remarkably, as in the heat engine case, we can produce configurations which approach $C_{op}^{(c)}$ with arbitrary precision while delivering maximum power exploiting the same 'energy filtering' dissipation rates. Before discussing this effect we present some universal properties of the CMP and we analyze the performance of the baths models of equation (9).

Assuming that the rates depend on the energy and on the temperature through the product $\beta\epsilon$, i.e. $\Gamma_\alpha(\epsilon_\alpha) = \Gamma_\alpha(\beta_\alpha\epsilon_\alpha)$ (e.g. the models (9) satisfy this hypothesis for $n = 0$, while they do not for $n > 0$), we find that the COP at maximum power reduces to the universal family of curves

$$\mathrm{C}_{op}(P_{[R]}^{\max}) = \mathrm{C}_{op}^{(0)}\mathrm{C}_{op}^{(c)}/(1 + \mathrm{C}_{op}^{(0)} + \mathrm{C}_{op}^{(c)}), \tag{12}$$

where $C_{op}^{(0)}$ represents the COP when $\beta_H = \beta_C$. It thus follows that for these models the knowledge of $C_{op}(P_{[R]}^{\max})$ at a single bath temperature configuration identifies unambiguously the COP for all other temperature differences. This feature is in contrast with the heat engine mode since, under the same hypothesis, the EMP at arbitrary temperatures depends on the details of the system.

Consider next the maximum power for the models described equation (9). We find that the maximization in equation (8) yields $\epsilon_H^* \to +\infty$ (and a finite value of ϵ_C^*), which implies

$$P_{[R]}^{(\max)} = c_n k_C/\beta_C^{n+1}, \qquad C_{op}(P_{[R]}^{\max}) = 0, \tag{13}$$

where c_n is a dimensionless number which only depends on n for $n > 0$, while it is a function of k_H/k_C if $n = 0$ (see appendix D for details). The fact that the corresponding COP is equal to zero is a direct consequence of the divergent value of ϵ_H^*: physically it means that the maximum cooling power (which is finite, see equation (13)) is obtained by performing an infinite work, thus by releasing an infinite amount of heat into the hot bath. In the more realistic scenario where there are limitations on our control of the gaps, say $|\epsilon_\alpha| \leqslant \Delta$, the resulting value of $P_{[R]}^{(\max)}$ will be smaller than in equation (13) but the associated COP will be non-zero with a scaling that for large enough Δ goes as $\mathrm{C}_{op}(P_{[R]}^{\max}) \propto 1/(\beta_C\Delta)$ (see appendix D for details). Equation (13) shows that in all models the maximum cooling power only depends on the temperature $1/\beta_C$ of the cold lead as a simple power law, and it vanishes as $1/\beta_C \to 0$. Intuitively this makes sense since it is harder to refrigerate a colder bath and at $1/\beta_C = 0$

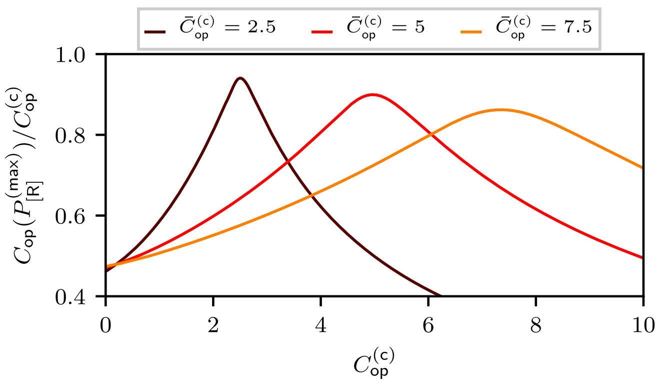

Figure 3. $C_{\rm op}(P_{[R]}^{(\max)})$ as a function of $C_{\rm op}^{(c)}$ (varied by fixing β_H and sweeping over β_C), computed using the same Lorentzian filtering rates discussed in figure 2. Fixing $\sigma = 0.01$ and $\bar{\epsilon}_C = 1$ as in figure 2(c), we choose $\bar{\epsilon}_H/\bar{\epsilon}_C = 7/5, 6/5$ and $17/15$, corresponding to bath temperature configurations $\bar{C}_{\rm op}^{(c)} = 2.5, 5$ and 7.5. Energies are expressed in units of $1/\beta_H$ and the CMP does not depend on γ.

there is no energy to extract from the bath. Furthermore, for $n > 0$ the properties of the hot bath (i.e. temperature and coupling constant) do not enter the $P_{[R]}^{(\max)}$ formula.

We now return to the possibility of having the CMP arbitrarily close to $C_{\rm op}^{(c)}$. As in the heat engine case, from the second equality of equation (11) we see that, if the maximization in equation (8) yields values of ϵ_H^* and ϵ_C^* such that $\epsilon_H^*\beta_H \approx \epsilon_C^*\beta_C$, then $C_{\rm op}(P_{[R]}^{\max}) \approx C_{\rm op}^{(c)}$. Indeed, as we can see in figure 3, we are able to have a CMP close to $C_{\rm op}^{(c)}$ at any desired temperature configuration $\bar{C}_{\rm op}^{(c)}$ by considering appropriately tuned Lorentzian rates (described in figure 2).

5. Thermal accelerator [A] and heater [H] modes

For the physical models described in equation (9) it turns out that in order to maximize the heat entering the cold bath, it is more convenient to release heat into both baths ($J_H, J_C < 0$), rather than extracting heat from the hot bath H and releasing it into the cold bath ($J_H > 0, J_C < 0$). The thermal accelerator mode [A] thus appears to be useless if we are just interested in maximizing the heat delivered to the cold bath. Accordingly, in the following we shall focus on the heater [H] mode only with a single bath (or equivalently with two baths at the same temperature). Assuming to have some physical limit $|\epsilon| \leqslant \Delta$ on the way we can control the gap, from equation (8) we find

$$P_{[H]}^{(\max)} = \frac{k\Delta^{n+1}}{2} \times \begin{cases} \tanh\dfrac{\beta\Delta}{2}, & (F_n \text{ model}), \\ 1, & (B_n \text{ model}), \end{cases} \tag{14}$$

where k is the coupling constant appearing in equation (9). Equation (14) shows that the maximum power diverges as $\Delta \to +\infty$, the exponent of Δ depending on the density of states associated with the rates. Interestingly, the maximum power that can be delivered to the bath vanishes for high temperatures ($\beta\Delta \ll 1$) in the fermionic models, while it is finite and insensitive to temperature in the bosonic models. This is due to the peculiar rates of the bosonic models which diverge for $\beta\epsilon \ll 1$. On the contrary, for low temperatures ($\beta\Delta \gg 1$) both models yield the same value of $P_{[H]}^{(\max)}$.

6. Finite-time corrections

The derivation of our main equation (8) was obtained under the implicit assumption that one could implement infinitesimal control cycles. Yet this hypothesis is not as crucial as it may appear. Indeed the feasibility of an infinitesimal Otto cycle relies on the ability of performing a very fast driving with respect to the typical time scales of the dynamics, a regime that can be achieved in several experimental setups [58, 59]. Furthermore by taking the square-wave protocol shown in figure 1(b) characterized by finite time intervals τ_H and τ_C still fulfilling the ratio $\tau_H/\tau_C = \sqrt{\Gamma_C(\epsilon_C)/\Gamma_H(\epsilon_H)}$, we find that, at leading order in dt, the maximum power $P_{[\nu]}^{(\max)}(\mathrm{d}t)$ only different from the ideal value $P_{[\nu]}^{(\max)}$ of equation (8) by a quadratic correction, i.e. $P_{[\nu]}^{(\max)}(\mathrm{d}t) \approx (1 - \tilde{\Gamma}_H\tilde{\Gamma}_C \mathrm{d}t^2/12)P_{[\nu]}^{(\max)}$, where $\tilde{\Gamma}_\alpha = (\tilde{\Gamma}\Gamma_\alpha)^{1/2}$, $\tilde{\Gamma} = \Gamma_H\Gamma_C/(\sqrt{\Gamma_H} + \sqrt{\Gamma_C})^2$, and all rates are computed for ϵ_H and ϵ_C that maximize equation (8). Besides, even in the regime where $\tilde{\Gamma}_H \mathrm{d}t$, $\tilde{\Gamma}_C \mathrm{d}t \gg 1$, $P_{[\nu]}^{(\max)}(\mathrm{d}t)$ can be shown (see appendix B for details) to only decrease as $(\tilde{\Gamma}_H \mathrm{d}t/2)^{-1} + (\tilde{\Gamma}_C \mathrm{d}t/2)^{-1}$, implying that a considerable fraction of $P_{[\nu]}^{(\max)}$ can still be achieved also in this case (e.g. see figure 1(c) where we report the dt dependence of $P_{[\mathrm{H}]}^{(\max)}(\mathrm{d}t)$ in the heater mode). On the contrary deviations from equation (8) due to finite time corrections in the quenches turns out to be more relevant. These last are first order in the ration between the duration of the quench (now different from 0) and the period of the protocol dt (see appendix B for details).

7. Conclusions

We proved that a cycle switching between two extremal values in the fast-driving regime achieves universally the maximum power and the maximum cooling rate (respectively for a working medium operating as a heat engine or as a refrigerator), regardless of the specific dissipation rates, and we found a general expression for the external control during the cycle. The power advantage of modulating the control fields with rapid adiabatic transformations has been observed in the literature [51, 68, 74] for some specific model and this intuition is in agreement with our general results. We also found that the first coefficient of the expansion in power of η_C of the EMP is universal while the second one is linked to the symmetry of the dissipation coefficients. This paper enlights that the features mentioned above are valid also strongly out of equilibrium, while already proven in low dissipation [64] and steady state [3] heat engines. If the bath spectral densities can be suitably tailored through energy filters (as for instance in [73]) our protocol allows to reach the Carnot bound at maximum power both operating as a heat engine or refrigerator, although at the cost of a vanishing power. This observation proves the lack of universal upper bounds to the EMP. Finally, a new scaling for the COP of a bath with flat spectral density is shown and a clear dependence of the EMP and the COP at maximum power on the spectral densities of the two thermal baths is established. The results are discussed in detail for some specific models, from flat bosonic and fermionic baths to environments with more complicated spectral densities, and finite driving speed effects are analyzed.

Acknowledgments

We thank G M Andolina for useful discussions. This work has been supported by SNS-WIS joint lab ‘QUANTRA’, by the SNS internal projects ‘Thermoelectricity in nano-devices’, and by the CNR-CONICET cooperation programme ‘Energy conversion in quantum, nanoscale, hybrid devices’.

Appendix A. Optimality of infinitesimal Otto cycles

In this appendix we present explicit proof that infinitesimal Otto cycles are optimal for reaching maximum power performances for our two-level setting. As a preliminary result we clarify that under periodic modulations of the control parameters, the master equation (equation (4) of the main text) produces solutions which asymptotically are also periodic. For this purpose let us write equation (4) of the main text as $\dot{p}(t) = A(t)p(t) + B(t)$ where, for ease of notation, we introduced the functions

$$A(t) = -\sum_{\alpha=\mathrm{H,C}} \lambda_\alpha(t)\Gamma_\alpha[\epsilon(t)], \qquad B(t) = \sum_{\alpha=\mathrm{H,C}} \lambda_\alpha(t)\Gamma_\alpha[\epsilon(t)]p_{\mathrm{eq}}^{(\alpha)}[\epsilon(t)], \tag{A.1}$$

and consider periodical driving forces such that $A(t+\tau) = A(t)$, $B(t+\tau) = B(t)$ for all t. By explicitly integration we get

$$p(t) = \int_0^t \mathrm{e}^{\int_{t'}^t A(t'')\mathrm{d}t''} B(t')\mathrm{d}t' + \mathrm{e}^{\int_0^t A(t')\mathrm{d}t'} p(0). \tag{A.2}$$

Decompose then the integral on the right-hand side as

$$\int_0^t \mathrm{e}^{\int_{t'}^t A(t'')\mathrm{d}t''} B(t')\mathrm{d}t' = \int_{t-\tau}^t \mathrm{e}^{\int_{t'}^t A(t'')\mathrm{d}t''} B(t')\mathrm{d}t' + \int_0^{t-\tau} \mathrm{e}^{\int_{t'}^{t-\tau} A(t'')\mathrm{d}t''} \mathrm{e}^{\int_{t-\tau}^t A(t'')\mathrm{d}t''} B(t')\mathrm{d}t'. \tag{A.3}$$

Notice now that, since $A(t)$ and $B(t)$ are periodic, the quantity $c(t) = \int_{t-\tau}^t \mathrm{e}^{\int_{t'}^t A(t'')\mathrm{d}t''} B(t')\mathrm{d}t'$ is also periodic with period τ, while $d = e^{\int_{t-\tau}^t A(t'')dt''}$ is constant in time. Substituting the previous definitions in equation (A.3) and then in equation (A.2) we find

$$p(t) = c(t) + d\int_0^{t-\tau} \mathrm{e}^{\int_{t'}^{t-\tau} A(t'')\mathrm{d}t''} B(t')\mathrm{d}t' + \mathrm{e}^{\int_0^t A(t')\mathrm{d}t'} p(0). \tag{A.4}$$

In the asymptotic limit where the initial condition $p(0)$ has been completely forgotten (since $A(t) \leqslant 0$ at all times, the contribution of the initial condition decays exponentially), equation (A.2) gives

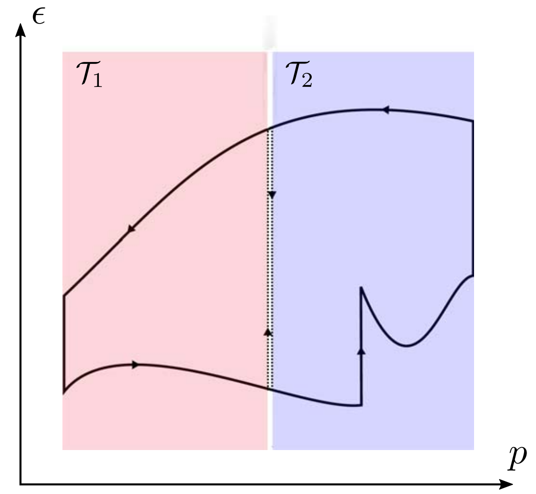

Figure A1. The original cycle is represented by a black line following a closed path in the (p, ϵ) plane. The two sub-cycles are the portions of the original one enclosed in the light red and in the light blue squares, respectively denoted with $\mathcal{T}_1$ and $\mathcal{T}_2$.

$$p(t-\tau) \approx \int_0^{t-\tau} e^{\int_{t'}^{t-\tau} A(t'')\mathrm{d}t''} B(t')\mathrm{d}t', \tag{A.5}$$

which substituted in equation (A.4) allows us to write

$$p(t) \approx c(t) + dp(t-\tau), \tag{A.6}$$

where we neglected again the contribution coming from the initial condition. Equation (A.6) defines a recursive succession, with limit point equal to $c(t)/(1-d)$, the periodicity of $c(t)$ concludes the proof. This result can also be framed in the general context of Floquet theory [75]. The Floquet theorem states that a fundamental matrix solution of a first order differential equation with periodically driven coefficients is quasi-periodical, namely can be written as $y(t) = P(t)e^{Mt}$ where $P(t)$ is a periodic matrix function (with the same period of the coefficients) and e^{Mt} is the so called *monodromy matrix*. The real parts of the eigenvalues of M are responsible of the asymptotic behavior of the solutions and are known as Lyapunov exponents, a stable cyclic solution is characterized by their negativity. In the case of equation (4) of the main text, our calculations reveal that the monodromy matrix is given by the constant d, the sign of the Lyapunov exponent is given by $\log d < 0$, confirming our predictions about the stability.

In the above paragraph we showed that the asymptotic solution of equation (4) of the main text is periodic with the same period of the external driving $\epsilon(t)$. Notice that in the equilibrium scenario the previous result is trivial, since the population instantly relaxes to the Gibbs state that is a monotonic function of the control parameter ϵ. In our case we can establish only that $p(t)$ and $\epsilon(t)$ share the same period, although finding the proper functional relation between the two is absolutely non-trivial (see for example [43]). However we don't need any additional information to prove that any cycle that is not infinitesimal, namely a square wave protocol in which the controls jump at a time much faster that the typical dynamical scale Γ, cannot achieve the maximum power. The proof is outlined in the following: since $\epsilon(t)$ and $p(t)$ share the same periodicity, a cycle can be represented in the (p, ϵ) plane as a closed curve. Let us suppose that the optimal cycle $\mathcal{T}$ is not infinitesimal, for example as in figure A1. Thus, it is possible to perform an instantaneous quench, for example, in the middle (where the probability is halfway between the minimum and maximum value), and divide the transformation in two smaller sub-cycles $\mathcal{T}_1$ and $\mathcal{T}_2$ (see figure A1). Since the quenches are instantaneous, they do not contribute to the heat exchanged and to the time duration of the process. Furthermore, performing the two sub-cycles in series effectively builds a transformation with the same average power of the original cycle, a property that in symbols we can exemplify as $P(\mathcal{T}) = P(\mathcal{T}_1 \circ \mathcal{T}_2)$. Simple calculations reveal that the power of the single sub-cycles cannot be both greater or smaller than the power of the original one, thus we are left with two possibilities, $P(\mathcal{T}_1) \leqslant P(\mathcal{T}_1 \circ \mathcal{T}_2) \leqslant P(\mathcal{T}_2)$ or $P(\mathcal{T}_2) \leqslant P(\mathcal{T}_1 \circ \mathcal{T}_2) \leqslant P(\mathcal{T}_1)$. In both cases the original cycle is sub-optimal, that is absurd, unless $P(\mathcal{T}_1) = P(\mathcal{T}_1 \circ \mathcal{T}_2) = P(\mathcal{T}_2)$ but even in this case we can choose one of the two sub-cycles still preserving optimality.

The previous argument shows that the only candidates for power maximization are those cycles that cannot be divided with a quench as done in the above proof, thus being infinitesimal. Notice that the previous proof strongly relies on the possibility of performing effectively instantaneous quenches, a characteristic that is better analyzed in the next appendix. At last, by using Pontryagin's minimum principle, it can be shown that if coupling constants $\lambda_{\mathrm{H}}(t)$ and $\lambda_{\mathrm{C}}(t)$ fulfill a 'trade-off relation' (i.e. if one increases, the other one decreases), then the optimal cycle will have $\lambda_C(t) = 0$ and $\lambda_H(t) = 1$, or $\lambda_C(t) = 0$ and $\lambda_H(t) = 1$ at all times [43]. This implies that the coupling to the baths must be switched during the quenches of the infinitesimal Otto-cycle.

Appendix B. Maximum power formula and finite-time corrections

In this appendix we prove equation (5) of the main text and discuss the finite-time corrections.

As as shown in the previous appendix, the optimal cycle *must* be an infinitesimal Otto cycle, so we consider a protocol (depicted in figure 1(b) of the main text) where $\epsilon(t) = \epsilon_H$, $\lambda_H = 1$ and $\lambda_C = 0$ for $t \in [0, \tau_H]$, and $\epsilon(t) = \epsilon_C$, $\lambda_H = 0$ and $\lambda_C = 1$ for $t \in [\tau_H, \tau_H + \tau_C]$. The optimal cycle and corresponding power will then be found by taking the limit $dt = \tau_H + \tau_C \to 0$ and maximizing over the free parameters ϵ_H, ϵ_C and τ_H/τ_C.

We proceed the following way: first we perform an exact calculation, for arbitrary τ_H and τ_C, of the heat rates $\langle J_H\rangle$, $\langle J_C\rangle$, averaged over one period, flowing out of the hot and cold bath respectively. Then, in the limit $dt \to 0$, we find the ratio τ_H/τ_C that maximizes the power and we find the corresponding expression of the maximum power, proving equation (5) of the main text and the optimal ratio condition

$$\tau_H/\tau_C = \sqrt{\Gamma_C(\epsilon_C)/\Gamma_H(\epsilon_H)}. \tag{B.1}$$

The instantaneous heat currents can be written in terms of the probability $p(t)$ by plugging the solution of equation (4) of the main text into equation (3) of the main text. We denoted with $p_H(t)$ and $p_C(t)$ the solution of equation (4) of the main text respectively in the time intervals $\mathcal{I}_H = [0, \tau_H]$ and $\mathcal{I}_C = [\tau_H, \tau_H + \tau_C]$. Since the control parameters (i.e. $\epsilon(t)$, $\lambda_H(t)$ and $\lambda_C(t)$) are constant in each interval, we have that

$$p_H(t) = He^{-\Gamma_H t} + p_{eq}^{(H)},\; p_C(t) = Ce^{-\Gamma_C t} + p_{eq}^{(C)}, \tag{B.2}$$

where H and C are two constants and where, for ease of notation, we introduced the symbols $\Gamma_\alpha := \Gamma_\alpha(\epsilon_\alpha)$ and $p_{eq}^{(\alpha)} := p_{eq}^{(\alpha)}(\epsilon_\alpha)$ (for $\alpha = H, C$). We determine the two constants H and C by imposing that the probability $p(t)$ is continuous in $t = \tau_H$, i.e.

$$p_H(\tau_H) = p_C(\tau_H) \tag{B.3}$$

and that $p(t)$ is periodic with period $\tau_H + \tau_C$, i.e.

$$p_H(0) = p_C(\tau_H + \tau_C). \tag{B.4}$$

We impose periodic boundary conditions because, as discussed in the previous appendix, a periodic protocol produces a periodic $p(t)$ after an initial transient time, and we are indeed interested in the 'asymptotic' regime. Equations (B.3) and (B.4) reduce to the following linear-algebra problem for the constants H and C:

$$\frac{1}{p_{eq}^{(C)} - p_{eq}^{(H)}}\begin{pmatrix} e^{-\Gamma_H\tau_H} & -e^{-\Gamma_C\tau_H} \\ 1 & -e^{-\Gamma_C(\tau_H+\tau_C)} \end{pmatrix}\begin{pmatrix} H \\ C \end{pmatrix} = \begin{pmatrix} 1 \\ 1 \end{pmatrix}, \tag{B.5}$$

with solution

$$\begin{pmatrix} H \\ C \end{pmatrix} = \frac{(p_{eq}^{(C)} - p_{eq}^{(H)})}{\sinh[(\Gamma_H\tau_H + \Gamma_C\tau_C)/2]}\begin{pmatrix} e^{\Gamma_H\tau_H/2}\sinh(\Gamma_C\tau_C/2) \\ -e^{\Gamma_C\tau_H}e^{\Gamma_C\tau_C/2}\sinh(\Gamma_H\tau_H/2) \end{pmatrix}, \tag{B.6}$$

which, via equation (B.2), completely determine $p(t)$. By substituting equation (B.2) into equation (3) of the main text, we can write the averaged heat rates $\langle J_H\rangle$ and $\langle J_C\rangle$ as

$$\begin{aligned} \langle J_H\rangle &:= \frac{1}{\tau_H + \tau_C}\int_{\mathcal{I}_H} J_H dt = \frac{\epsilon_H}{\tau_H + \tau_C}\int_{\mathcal{I}_H}\dot{p}_H dt = \frac{\epsilon_H H}{\tau_H + \tau_C}[e^{-\Gamma_H\tau_H} - 1], \\ \langle J_C\rangle &:= \frac{1}{\tau_H + \tau_C}\int_{\mathcal{I}_C} J_C dt = \frac{\epsilon_C}{\tau_H + \tau_C}\int_{\mathcal{I}_C}\dot{p}_C dt = \frac{\epsilon_C C}{\tau_H + \tau_C}e^{-\Gamma_C\tau_H}[e^{-\Gamma_C\tau_C} - 1], \end{aligned} \tag{B.7}$$

where we use the fact that $\epsilon(t)$ is constant in each $\mathcal{I}_\alpha$ and the fact that, since the two-level system is coupled to one bath at a time, $\dot{p}_\alpha = \dot{p}$ with $p(t) = p_H(t)$ during $\mathcal{I}_H$ and $p(t) = p_C(t)$ during $\mathcal{I}_C$. Using the expressions for H and C given in equation (B.6), we can rewrite equation (B.7) as

$$\langle J_{H/C}\rangle = \pm\frac{\epsilon_{H/C}}{\tau_H + \tau_C}\frac{\Gamma_H\tau_H\Gamma_C\tau_C}{\Gamma_H\tau_H + \Gamma_C\tau_C}(p_{eq}^{(H)} - p_{eq}^{(C)})\frac{(\Gamma_H\tau_H/2)^{-1} + (\Gamma_C\tau_C/2)^{-1}}{\coth(\Gamma_H\tau_H/2) + \coth(\Gamma_C\tau_C/2)}. \tag{B.8}$$

We now impose that $dt = \tau_H + \tau_C$ by setting $\tau_H = \theta dt$ and $\tau_C = (1 - \theta)dt$, for $\theta \in [0, 1]$, in equation (B.8). Taking hence the infinitesimal cycle limit $dt \to 0$ we get

$$\langle J_{H/C}\rangle = \pm\epsilon_{H/C}\frac{\Gamma_H\theta\;\Gamma_C(1 - \theta)}{\Gamma_H\theta + \Gamma_C(1 - \theta)}(p_{eq}^{(H)} - p_{eq}^{(C)}). \tag{B.9}$$

The maximization over θ of the above expression yields the condition

$$\frac{\theta}{1-\theta} = \sqrt{\frac{\Gamma_C}{\Gamma_H}}, \tag{B.10}$$

which, multiplying by dt the numerator and the denominator of the left-hand side of equation (B.10), proves equation (B.1). Solving hence equation (B.10) for θ and plugging the result into equation (B.9) yields

$$\langle J_{H/C}\rangle = \pm\epsilon_{H/C}\frac{\Gamma_H\Gamma_C}{(\sqrt{\Gamma_H}+\sqrt{\Gamma_C})^2}(p_{eq}^{(H)} - p_{eq}^{(C)}), \tag{B.11}$$

which replaced into equation (1) of the main text, and maximizing with respect to the only two free parameters left, i.e. ϵ_H and ϵ_C, allows us to derive equation (5) of the main text for all four thermal machine modes. An additional comment has to be made for the accelerator mode [A], that aims at maximizing the heat released into the cold bath while extracting heat from the hot bath. By definition, we must restrict the maximization in equation (5) of the main text to guarantee $\langle J_H\rangle \geqslant 0$, e.g. by forcing $\mathcal{C}$ to be $(\epsilon_H \geqslant 0 \cap \beta_C\epsilon_C \geqslant \beta_H\epsilon_H) \cup (\epsilon_H \leqslant 0 \cap \beta_C\epsilon_C \leqslant \beta_H\epsilon_H)$. On the other hand, the heater mode consists of heating a single reservoir whose interaction with the two-level system is described by a rate $\Gamma(\epsilon)$ and equilibrium probability $p_{eq}(\epsilon)$. So in this case the maximization must be performed taking $\Gamma_\alpha(\epsilon) = \Gamma(\epsilon)$ and $p_{eq}^{(\alpha)}(\epsilon) = p_{eq}(\epsilon)$ (for $\alpha = H, C$). If we also require that $\Gamma(\epsilon) = \Gamma(-\epsilon)$, which physically means that the rates do not distinguish which one of the two energy levels is the ground and excited state, we find that equation (5) can be simplified to

$$P_{[H]}^{(max)} = \max_{\epsilon\geqslant 0,\epsilon\in\mathcal{C}} \frac{1}{2}\epsilon\,\Gamma(\epsilon)[1-2p_{eq}(\epsilon)], \tag{B.12}$$

and the corresponding optimal cycle is given by an Otto cycle where $\tau_H = \tau_C$ and the value ϵ that maximizes equation (B.12) determines $\epsilon_H = -\epsilon_C = \epsilon$. Thus the optimal cycle in the heater case corresponds to attempting continuous population inversions.

B.1. Finite-time corrections part one

Setting $\tau_H = \theta dt$ and $\tau_C = (1-\theta)dt$ in equation (B.8), and plugging in the expression of θ that satisfies equation (B.10), we find that the average heat rate for an arbitrary period dt is given by

$$\langle J_{H/C}(dt)\rangle = \pm\epsilon_{H/C}\frac{\Gamma_H\Gamma_C}{(\sqrt{\Gamma_H}+\sqrt{\Gamma_C})^2}(p_{eq}^{(H)} - p_{eq}^{(C)})\frac{(\tilde{\Gamma}_H dt/2)^{-1} + (\tilde{\Gamma}_C dt/2)^{-1}}{\coth(\tilde{\Gamma}_H dt/2) + \coth(\tilde{\Gamma}_C dt/2)}, \tag{B.13}$$

where $\tilde{\Gamma}_\alpha = (\tilde{\Gamma}\Gamma_\alpha)^{1/2}$ and $\tilde{\Gamma} = \Gamma_H\Gamma_C/(\sqrt{\Gamma_H}+\sqrt{\Gamma_C})^2$. Plugging this results into equation (1) of the main text and maximizing over ϵ_H and ϵ_C yields the expression

$$P_{[\nu]}^{(max)}(dt) = \frac{(\tilde{\Gamma}_H dt/2)^{-1} + (\tilde{\Gamma}_C dt/2)^{-1}}{\coth(\tilde{\Gamma}_H dt/2) + \coth(\tilde{\Gamma}_C dt/2)} P_{[\nu]}^{(max)}, \tag{B.14}$$

which provides the finite time version of equation (5) of the main text. On one hand, as anticipated in the main text, by expanding equation (B.14) for small dt, we find the following quadratic correction

$$P_{[\nu]}^{(max)}(dt) \approx (1 - \tilde{\Gamma}_H\tilde{\Gamma}_C dt^2/12)P_{[\nu]}^{(max)}. \tag{B.15}$$

On the other hand for $\tilde{\Gamma}_H t$, $\widetilde{d\Gamma}_C t \gg 1$, we get

$$P_{[\nu]}^{(max)}(dt) \approx \frac{(\tilde{\Gamma}_H dt/2)^{-1} + (\tilde{\Gamma}_C dt/2)^{-1}}{2} P_{[\nu]}^{(max)}, \tag{B.16}$$

implying that a considerable fraction of $P_{[\nu]}^{(max)}$ can be achieved even if the driving frequency is slower than the typical rate. Notice that equation (B.14) is a strictly decreasing function of dt; this is consistent with the fact that an infinitesimal cycle is indeed the optimal solution.

We conclude by observing that we can simplify equation (B.14) for the heater mode where a single reservoir is coupled to the two-level system. Under the hypothesis leading to equation (B.12), we find that

$$P_{[H]}^{(max)}(dt) = \frac{\tanh(dt\Gamma/4)}{dt\Gamma/4}P_{[H]}^{(max)}, \tag{B.17}$$

where Γ is computed in the value of ϵ that maximizes equation (B.12). Figure 1(c) of the main text, which is a plot of equation (B.17), shows that $P_{[H]}^{(max)}(dt) \approx P_{[H]}^{(max)}$ up to $dt\Gamma \approx 2$, while for $dt\Gamma = 10 \gg 1$, $P_{[H]}^{(max)}(dt)$ is only decreased of a factor two.

B.2. Finite-time corrections part two: the quenches

Finite-time corrections to the power may not only arise from the finite duration of the isothermal transformations (i.e. from a finite value of τ_C and τ_H), but also from a finite duration τ of the quenches, i.e. of the transformations during which ϵ changes between the two extremal values ϵ_C and ϵ_H. We will thus assume that each quench is carried out in a time τ. The aim of this appendix is to show how these effects could be accounted for, and to estimate the leading order corrections to the maximum power delivered by the heat engine due to this effect; analogous considerations hold also for the other machines. We will thus restrict ourself to the regime $\tau \ll dt \ll \gamma^{-1}$, where $dt = \tau_C + \tau_H$ and γ is the characteristic rate of the system during the protocol. The first inequality states that the duration of the quenches is much smaller than the duration of the isothermal transformations. The second inequality implies that the finite-time corrections discussed in the previous subsection are neglected, since they have been previously discussed.

Using the results of appendix A, we know that $p(t)$ has a limit cycle with the same period of $\epsilon(t)$. If we further assume that the protocol is much faster than γ, the probability tends to a fixed value $\bar{p}$ given by

$$\bar{p} = \frac{\int_0^T ds \Gamma(s) p_{eq}(s)}{\int_0^T ds \Gamma(s)}, \tag{B.18}$$

where $T = dt + 2\tau$ is the total duration of the protocol, $\Gamma(s) = \lambda_H(s)\Gamma_H[\epsilon(s)] + \lambda_C(s)\Gamma_C[\epsilon(s)]$ and

$$p_{eq}(s) = \frac{\lambda_H(s)\Gamma_H[\epsilon(s)] p_{eq}^{(H)}[\epsilon(s)] + \lambda_C(s)\Gamma_C[\epsilon(s)] p_{eq}^{(C)}[\epsilon(s)]}{\lambda_H(s)\Gamma_H[\epsilon(s)] + \lambda_C(s)\Gamma_C[\epsilon(s)]}. \tag{B.19}$$

By using again the hypothesis that the protocol is much faster than γ, we can write the power of the heat engine, averaged over one period, as

$$P_{[E]}(\lambda) = \frac{1}{T}\int_0^T ds\ \epsilon(s)\Gamma(s)[p_{eq}(s) - \bar{p}]. \tag{B.20}$$

As in the ideal protocol (see figure 1(b) of the main text), we will assume that during the two isothermal transformations we respectively have $\epsilon(s) = \epsilon_H$, $\lambda_H(s) = 1$, $\lambda_C(s) = 0$ and $\epsilon(s) = \epsilon_C$, $\lambda_H(s) = 0$, $\lambda_C(s) = 1$. This means that we are coupled to one bath at a time. Instead, during the quenches we assume that all three control parameters ($\epsilon(s)$, $\lambda_H(s)$ and $\lambda_C(s)$) vary linearly in time between the corresponding extremal values. We thus divide the integral in equation (B.20) in the four different transformations:

$$\begin{aligned} P_{[E]}(\tau) &= \frac{\int_0^{\tau_H}(\ldots) + \int_{\tau_H}^{\tau_H+\tau}(\ldots) + \int_{\tau_H+\tau}^{\tau_H+\tau_C+\tau}(\ldots) + \int_{\tau_H+\tau_C+\tau}^{\tau_H+\tau_C+2\tau}(\ldots)}{dt + 2\tau} \\ &\equiv \frac{\mathcal{W}_H + \mathcal{W}_{H\to C} + \mathcal{W}_C + \mathcal{W}_{C\to H}}{dt + 2\tau}, \end{aligned} \tag{B.21}$$

where $(\ldots)$ stands for $ds\ \epsilon(s)\Gamma(s)[p_{eq}(s) - \bar{p}]$. In the regime we consider the power, up to leading order corrections in τ/dt, can be written as

$$P_{[E]}(\tau) = \frac{\mathcal{W}_H + \mathcal{W}_C}{dt}\left(1 - \frac{2\tau}{dt}\right) + \frac{\mathcal{W}_{H\to C} + \mathcal{W}_{C\to H}}{dt}, \tag{B.22}$$

where the first addend is obtained by means of a first order expansion in τ/dt of the denominator in the rhs of equation (B.21).

We wish to compare equation (B.22) to the power $P_{[E]}^{(max)}$ achieved in the ideal protocol, so we will estimate the four terms $\mathcal{W}_H$, $\mathcal{W}_C$, $\mathcal{W}_{H\to C}$ and $\mathcal{W}_{C\to H}$. First, we notice that $\bar{p}$ depends on the whole protocol, see equation (B.18). We can thus write

$$\bar{p} = \bar{p}^{(0)} + \delta\bar{p}^{(1)}, \tag{B.23}$$

where $\bar{p}^{(0)}$ is the value of $\bar{p}$ in the ideal protocol, and $\delta\bar{p}^{(1)}$ the corrections due to the finite-time quenches. These two terms can be calculated simply by dividing the integrals in the definition of $\bar{p}$ as we did for $P_{[E]}(\tau)$. It is easy to see that $\delta\bar{p}^{(1)}$ is of the order τ/dt. Since $\mathcal{W}_H$ and $\mathcal{W}_C$ are linear functions of $\bar{p}$, and $\bar{p} = \bar{p}^{(0)} + \delta\bar{p}^{(1)}$, we have that, for $\alpha = H, C$

$$\mathcal{W}_\alpha = \tau_\alpha \epsilon_\alpha \Gamma_\alpha(\epsilon_\alpha)[p_{eq}^{(\alpha)}(\epsilon_\alpha) - \bar{p}] = \mathcal{W}_\alpha^{(0)} + \mathcal{W}_\alpha^{(1)}, \tag{B.24}$$

where $\mathcal{W}_\alpha^{(0)}$ is the work extracted in the ideal protocol during the isothermal transformation, while $\mathcal{W}_\alpha^{(1)}$ represents the corrections due to the variation in population $\bar{p}$ induced by the finite-time quenches. We have that

$$\mathcal{W}_\alpha^{(1)} = -\tau_\alpha \epsilon_\alpha \Gamma_\alpha(\epsilon_\alpha)\delta\bar{p}^{(1)} \propto \epsilon_\alpha O(\gamma\tau), \tag{B.25}$$

where the last term means that $\mathcal{W}_\alpha^{(1)}$ is of the order $\gamma\tau$.

Next, we need to estimate $\mathcal{W}_{H\to C}$ and $\mathcal{W}_{C\to H}$. By inspecting the definition, we see that

$$\mathcal{W}_{H\to C} = \mathcal{W}_{C\to H} \propto \langle\epsilon\rangle O(\gamma\tau), \tag{B.26}$$

where $\langle\epsilon\rangle$ is a characteristic value of the energy gap during the quench.

Now we can return to equation (B.22). Using equations (B.24)–(B.26), and noticing that the order of magnitude of $\gamma\langle\epsilon\rangle$ is the same as $P_{[E]}^{(\max)}$, we find that all the corrections previously discussed are of the order γ/dt. We thus conclude that

$$P_{[E]}(\tau) = P_{[E]}^{(\max)}[1 - O(\tau/dt)], \tag{B.27}$$

where the corrections must be negative by virtue of the theorem proved in appendix A. The impact of finite time quenches is thus first order τ/dt.

Appendix C. Efficiency at maximum power

For small temperature differences, i.e. for small values of η_c, we can consider an expansion of the EMP of the kind

$$\eta(P_{[E]}) = a_1\eta_c + a_2\eta_c^2 + \dots. \tag{C.1}$$

In this appendix we prove that $a_1 = 1/2$, while for symmetric or constant rates we further have $a_2 = 1/8$. The maximum power of a heat engine (without constraints on the control parameters) can be written as (see equation (5) of the main text)

$$P_{[E]}^{(\max)} = \max_{(x_H, x_C)} P_{[E]}(x_H, x_C), \tag{C.2}$$

where

$$P_{[E]}(x_H, x_C) := \frac{g(x_H, x_C; \eta_c)}{\beta_H}[x_H - x_C(1 - \eta_c)][f(x_H) - f(x_C)], \tag{C.3}$$

$x_\alpha = \epsilon_\alpha\beta_\alpha$ (for $\alpha = \mathrm{H, C}$), $f(x) := [1 + \exp(x)]^{-1}$ and, expressing the Γ_α as a function of the gap ϵ and of the inverse temperature β_α of lead α

$$g(x_H, x_C; \eta_c) := \frac{\Gamma_H(x_H, \beta_H)\Gamma_C(x_C, \beta_H/(1 - \eta_c))}{(\sqrt{\Gamma_H(x_H, \beta_H)} + \sqrt{\Gamma_C(x_C, \beta_H/(1 - \eta_c))})^2}. \tag{C.4}$$

In equation (C.4) we decide to express β_C as $\beta_H/(1 - \eta_c)$ because we are interested in performing an expansion in η_c around a single inverse temperature β_H. Let x_H^* and x_C^* be respectively the values of x_H and x_C that maximize $P_{[E]}(x_H, x_C)$. By inspecting equations (C.3) and (C.4), we see that x_α^* is a function of η_c (and of β_H through g), so we can express x_α^* as a power series in η_c:

$$\begin{aligned} x_H^* &= m_0 + m_1\eta_c + m_2\eta_c^2 + \dots, \\ x_C^* &= m_0 + n_1\eta_c + n_2\eta_c^2 + \dots. \end{aligned} \tag{C.5}$$

Both x_H^* and x_C^* have the same leading order term. This can be seen considering equation (C.3) at $\eta_c = 0$: $g(x_H, x_C; 0)/\beta_H \geqslant 0$, while $[x_H - x_C][f(x_H) - f(x_C)] \leqslant 0$, so the maximum power is zero (at equal temperatures, the second law forbids the possibility of extracting work). Inspecting equation (C.3), it is easy to see that zero power at $\eta_c = 0$ implies $x_H = x_C$. Using equation (7) of the main text, we have that

$$\eta(P_{[E]}^{(\max)}) = 1 - \frac{x_C^*}{x_H^*}(1 - \eta_c), \tag{C.6}$$

so plugging equation (C.5) into (C.6) and expressing $\eta(P_{[E]}^{(\max)})$ as a power series in η_c, we find that

$$\eta(P_{[E]}^{(\max)}) = (1 + b_1)\eta_c + \frac{1}{2}(1 + b_2)\eta_c^2, \tag{C.7}$$

where

$$b_1 = \frac{m_1 - n_1}{m_0}, \qquad b_2 = \frac{m_1}{m_0} + 2\frac{m_2 - n_2}{m_0}.$$

Thus, the knowledge of b_1 and b_2 implies also the knowledge of a_1 and a_2. Also the maximum power $P_{[E]}(x_H^*, x_C^*)$ can be written as a power series in η_c by plugging the expansion equation (C.5) into (C.3). This yields

$$P_{[E]}(x_H^*, x_C^*) = \frac{1}{\beta_H}\sum_{n=0}^{+\infty} P_{[E]}^{(n)}\eta_c^n, \tag{C.8}$$

where the coefficients $P_{[E]}^{(n)}$ are functions of m_i, n_i (for $i = 0, 1, 2, \dots$) and of β_H. We now wish to determine b_1 and b_2 by maximizing $P_{[E]}^{(n)}$, starting from the lowest orders. We find that $P_{[E]}^{(0)} = P_{[E]}^{(1)} = 0$ and

$$P^{(2)}_{[E]} = \left[-\frac{b_1(1+b_1)}{2}\right]\frac{m_0^2\, g(m_0,\, m_0;\, 0)}{1+\cosh m_0}, \tag{C.9}$$

where we expressed n_1 in terms of b_1. The last fraction in equation (C.9) is positive, so $P^{(2)}_{[E]}$ is maximized by choosing b_1 that maximizes the term in square brackets, and m_0 that maximizes the last fraction. The maximization of the first term yields $b_1 = -1/2$, which readily implies (see equation (C.7)) $a_1 = 1/2$, as we wanted to prove. The maximization of the second term allows us to find the following implicit expression for m_0

$$g(m_0,\, m_0;\, 0)\left[2 - m_0 \tanh\left(\frac{m_0}{2}\right)\right] + m_0[\partial_{x_{\rm H}} g(m_0,\, m_0;\, 0) + \partial_{x_{\rm C}} g(m_0,\, m_0;\, 0)] = 0, \tag{C.10}$$

where $\partial_{x_\alpha} g(m_0,\, m_0;\, 0)$ denotes the partial derivative of $g(x_{\rm H}, x_{\rm C}; \eta_c)$, respect to x_α, calculated in $x_{\rm H} = x_{\rm C} = m_0$ and $\eta_c = 0$. In order to compute b_2, we must maximize also higher order terms of the power. It turns out that $P^{(3)}_{[E]}$ only depends on m_0 if we impose that $b_1 = -1/2$ and that m_0 satisfies equation (C.10). Thus, there is nothing to optimize, so we must analyze the next order. $P^{(4)}_{[E]}$ is a function of m_0, m_1, n_1, m_2, n_2 and $\beta_{\rm C}$. We write m_1 in terms of b_2, which is the only coefficient that determines a_2. We further express n_1 in terms of b_1, and impose $b_1 = -1/2$. At last, we write $g(m_0, m_0; 0)$ in terms of its partial derivatives using equation (C.10). This leads to an expression of $P^{(4)}_{[E]}$ as a function of m_0 (which is implicitly known), b_2, m_2, n_2 and $\beta_{\rm H}$. We maximize $P^{(4)}_{[E]}$ by setting to zero both partial derivatives of $P^{(4)}_{[E]}$ respect to b_2 and m_2. We thus find the following expression for b_2:

$$b_2 = \frac{m_0 \tanh\left(\frac{m_0}{2}\right)}{8}\cdot\frac{\partial_{x_{\rm H}} g - \partial_{x_{\rm C}} g}{\partial_{x_{\rm H}} g + \partial_{x_{\rm C}} g} - \frac{2\partial_{x_{\rm H}} g + \partial_{x_{\rm C}} g}{2(\partial_{x_{\rm H}} g + \partial_{x_{\rm C}} g)}, \tag{C.11}$$

where all partial derivatives of g are computed in $x_{\rm H} = x_{\rm C} = m_0$ and $\eta_c = 0$. This is, in principle, a closed expression for b_2, thus for a_2, since m_0 is defined in equation (C.10), and equation (C.11) only depends on m_0. Equation (C.11) shows that in general b_2, thus a_2, will depend on the specific rates. However, if $\partial_{x_{\rm H}} g = \partial_{x_{\rm C}} g$, the first term in equation (C.11) vanishes, while the second one reduces to a number, yielding $b_2 = -3/4$. Indeed, plugging this value of b_2 into equation (C.7) yields precisely $a_2 = 1/8$. We conclude the proof by noticing that if the rates are symmetric, i.e. $\Gamma_{\rm H}(\epsilon,\, \beta) = \Gamma_{\rm C}(\epsilon,\, \beta)$, $g(x_{\rm H},\, x_{\rm C};\, 0)$ is a symmetric function upon exchange of $x_{\rm H}$ and $x_{\rm C}$. This implies that $\partial_{x_{\rm H}} g(m_0,\, m_0;\, 0) = \partial_{x_{\rm C}} g(m_0,\, m_0;\, 0)$, so $a_2 = 1/8$. At last, if the rates are constants, also $g(x_{\rm H}, x_{\rm C}; \eta_c)$ is constant, trivially satisfying $\partial_{x_{\rm H}} g = \partial_{x_{\rm C}} g = 0$.

Appendix D. COP at maximum power

In this appendix we prove equations (9) and (10) of the main text and we derive the scaling of the COP at maximum power for large values of the maximum gap Δ given by $C_{\rm op}(P^{\rm max}_{[R]}) \propto 1/(\beta_{\rm C}\Delta)$. The COP at maximum power can be written as (see equation (8) of the main text)

$$C_{\rm op}(P^{\rm max}_{[R]}) = \frac{\epsilon^*_{\rm C}}{\epsilon^*_{\rm H} - \epsilon^*_{\rm C}}, \tag{D.1}$$

where $\epsilon^*_{\rm H}$ and $\epsilon^*_{\rm C}$ are respectively the values of $\epsilon_{\rm H}$ and $\epsilon_{\rm C}$ that maximize (see equation (5) of the main text)

$$P_{[R]}(\epsilon_{\rm H},\, \epsilon_{\rm C}) := -g(\epsilon_{\rm H},\, \epsilon_{\rm C})\epsilon_{\rm C}[f(\beta_{\rm H}\epsilon_{\rm H}) - f(\beta_{\rm C}\epsilon_{\rm C})], \tag{D.2}$$

where $f(x) := [1 + \exp(x)]^{-1}$ and

$$g(\epsilon_{\rm H},\, \epsilon_{\rm C}) := \frac{\Gamma_{\rm H}(\epsilon_{\rm H})\Gamma_{\rm C}(\epsilon_{\rm C})}{(\sqrt{\Gamma_{\rm H}(\epsilon_{\rm H})} + \sqrt{\Gamma_{\rm C}(\epsilon_{\rm C})})^2}. \tag{D.3}$$

We first prove that the COP at maximum power takes the universal form of equation (9) of the main text if the rates depend on the energy and on the temperature only through $\beta\epsilon$, i.e. $\Gamma_\alpha(\epsilon) = \Gamma_\alpha(\beta_\alpha \epsilon_\alpha)$. We rewrite equation (D.1) as a function of $x^*_\alpha = \beta_\alpha \epsilon^*_\alpha$ (for α = H, C):

$$C_{\rm op}(P^{\rm max}_{[R]}) = \left[\frac{x^*_{\rm H}}{x^*_{\rm C}}\left(\frac{1}{C^{(c)}_{\rm op}} + 1\right) - 1\right]^{-1}, \tag{D.4}$$

where $C^{(c)}_{\rm op}$ is the Carnot COP for a refrigerator (see main text). We can determine x^*_α by maximizing

$$P_{[R]}(x_{\rm H},\, x_{\rm C}) := -\frac{1}{\beta_{\rm C}}\frac{\Gamma_{\rm H}(x_{\rm H})\Gamma_{\rm C}(x_{\rm C})}{(\sqrt{\Gamma_{\rm H}(x_{\rm H})} + \sqrt{\Gamma_{\rm C}(x_{\rm C})})^2} x_{\rm C}[f(x_{\rm H}) - f(x_{\rm C})]. \tag{D.5}$$

Crucially, given our hypothesis on the rates, there is no explicit dependence on the temperatures in equation (D.5) (except for the prefactor $1/\beta_{\rm C}$), so the maximization of $P_{[R]}(x_{\rm H}, x_{\rm C})$ will simply yield two values of $x^*_{\rm H}$ and $x^*_{\rm C}$ that do not depend on the temperatures. Thus, for all bath temperatures the COP at maximum power will be given by equation (D.4), where $x^*_{\rm H}$ and $x^*_{\rm C}$ are two fixed values. The ratio $x^*_{\rm H}/x^*{}_{\rm C}$ will depend on the specific rates we consider. By imposing in equation (D.4) that the COP at maximum power of the system for $\beta_H = \beta_C$ (i.e. for $C_{op}^{(c)} \to \infty$) is $C_{op}^{(0)}$, we can eliminate the ratio $x_H^*/x^*{}_C$ in favor of $C_{op}^{(0)}$, concluding the proof of equation (9) of the main text.

We now prove equation (10) of the main text. Since equation (D.2) remains unchanged by sending both $\epsilon_H \to -\epsilon_H$ and $\epsilon_C \to -\epsilon_C$, we can assume without loss of generality that $\epsilon_C \geqslant 0$ (this is a general property which applies independently of the specific choice of bath models). Furthermore, we must ensure that the system is acting as a refrigerator by imposing $P_{[R]}(\epsilon_H, \epsilon_C) \geqslant 0$. This implies that $f(\beta_H \epsilon_H) \leqslant f(\beta_C \epsilon_C)$, thus

$$0 \leqslant \beta_C \epsilon_C \leqslant \beta_H \epsilon_H. \tag{D.6}$$

We now show that in the models described by equation (6) of the main text, the partial derivative of $P_{[R]}(\epsilon_H, \epsilon_C)$ respect to ϵ_H is non-negative for all values of ϵ_H and ϵ_C satisfying equation (D.6), which implies that $\epsilon_H^* \to +\infty$. Using equation (D.6), the condition $\partial P_{[R]}(\epsilon_H, \epsilon_C)/\partial \epsilon_H \geqslant 0$ can be written as

$$\frac{\partial}{\partial \epsilon_H} \ln g(\epsilon_H, \epsilon_C) \geqslant -\frac{\beta_H}{2[1 + \cosh(\beta_H \epsilon_H)]}. \tag{D.7}$$

Since $\partial \ln g(\epsilon_H, \epsilon_C)/\partial \epsilon_H$ has the same sign as $d\Gamma_H(\epsilon_H)/d\epsilon_H$, and since the rhs of equation (D.7) is strictly negative, equation (D.7) is certainly satisfied whenever $\Gamma_H(\epsilon_H)$ is a growing function. This proves that $\epsilon_H^* \to +\infty$ when the baths are described by the F_n model (see equation (6) of the main text) even when the two baths have different powers n. The B_n model is more tricky to analyze since the rates are decreasing functions around the origin. Nonetheless, using equation (D.6) it is possible to show that equation (D.7) is satisfied also in the B_n model by plugging $\Gamma_\alpha^{(B_n)}(\epsilon)$ (see equation (6) of the main text) into equation (D.7). This result holds also when the two baths have different powers n.

We now know that $\epsilon_H^* \to +\infty$ in the F_n and B_n models. Since both $\Gamma_H^{(F_n)}(\epsilon)$ and $\Gamma_H^{(B_n)}(\epsilon)$ diverge for $n > 0$ when $\epsilon_H^* \to +\infty$, we have that

$$g(+\infty, \epsilon_C) = \Gamma_C(\epsilon_C) = k_C\, \epsilon_C^n\, h(\beta_C \epsilon_C) = k_C \frac{x_C^n}{\beta_C^n} h(x_C), \tag{D.8}$$

where, as before, $x_C = \beta_C \epsilon_C$ and $h(x) := 1$ for the F_n model and $h(x) := \coth x/2$ for the B_n model (see equation (6) of the main text). Thus, using x_C instead of ϵ_C, and noting that $f(\epsilon_H \beta_H)$ vanishes for $\epsilon_H \to +\infty$, we can write $P_{[R]}(+\infty, \epsilon_C)$ [see equation (D.2)] as

$$P_{[R]}^{(n>0)} = \frac{k_C}{\beta_C^{n+1}} x_C^{n+1} h(x_C) f(x_C). \tag{D.9}$$

Equation (D.9) is non-negarive for all values of x_C and it vanishes in $x_C = 0$ and $x_C \to +\infty$ thanks to the exponential decrease of $f(x_C)$ for large values of x_C. Therefore, equation (D.9) will be maximum for the finite value x_C^* that maximizes $x_C^{n+1} h(x_C) f(x_C)$, and plugging x_C^* into equation (D.9) yields the first relation in equation (10) of the main text, where $c_n = (x_C^*)^{n+1} h(x_C^*) f(x_C^*)$. For $n = 0$, we separately analyze the F_0 and B_0 models. In the F_0 model, $g(\epsilon_H, \epsilon_C) = k_H k_C/(\sqrt{k_H} + \sqrt{k_C})^2$, so $P_{[R]}(+\infty, \epsilon_C)$ can be written as

$$P_{[R]}^{(F_0)} = \frac{k_C}{\beta_C} \frac{r}{(\sqrt{r} + 1)^2} x_C f(x_C), \tag{D.10}$$

where $r := k_H/k_C$. Using the same argument as before, equation (D.10) implies a finite value of x_C^* which arises from the maximization of $x_C f(x_C)$. We thus proved the first relation in equation (10) of the main text for the F_0 model, where $c_0 = r/(\sqrt{r} + 1)^2\, x_C^* f(x_C^*)$. At last, in the B_0 model $g(\epsilon_H \to +\infty, \epsilon_C) = k_H k_C \coth(x_C/2)/[\sqrt{k_H} + \sqrt{k_C \coth(x_C/2)}\,]^2$. Thus, $P_{[R]}(+\infty, \epsilon_C)$ can be written as

$$P_{[R]}^{(B_0)} = \frac{k_C}{\beta_C} \frac{r \coth(x_C/2)}{(\sqrt{r} + \sqrt{\coth(x_C/2)}\,)^2} x_C f(x_C). \tag{D.11}$$

Again, x_C^* is a finite value which can be found by maximizing $r \coth(x_C/2)\big/(\sqrt{r} + \sqrt{\coth(x_C/2)}\,)^2\ x_C f(x_C)$. Only in this case, x_C^* depends on the ratio r. We thus proved the first relation in equation (10) of the main text for the B_0 model, where $c_0 = r \coth(x_C^*/2)\big/(\sqrt{r} + \sqrt{\coth(x_C^*/2)}\,)^2\ x_C^* f(x_C^*)$.

The second relation in equation (10) of the main text stems from the fact that in all models $\epsilon_H^* \to +\infty$ while $\epsilon_C{}^*$ is finite. Thus, equation (D.1) implies that the $C_{op}(P_{[R]}^{max})$ vanishes. At last we want to roughly estimate the behavior of $C_{op}(P_{[R]}^{max})$ in the presence of a large yet finite constraint on the maximum gap: $|\epsilon(t)| \leqslant \Delta$. Since ϵ_H would diverge if there was no constraint, we can assume that, in the presence of Δ, $\epsilon_H^* = \Delta$. On the other hand, ϵ_C^* is a finite quantity (which is given by $\epsilon_C^* = x_C^*/\beta_C$ in the unconstrained case), so if we assume that $\Delta \gg \epsilon_C^*$, from equation (D.1) we have that

$$C_{\rm op}(P_{[\rm R]}^{\rm max}) \approx \frac{\epsilon_{\rm C}^*}{\epsilon_{\rm H}^*} \approx \frac{x_{\rm C}^*}{\beta_{\rm C}\Delta} \propto \frac{1}{\beta_{\rm C}\Delta}. \quad \text{(D.12)}$$

ORCID iDs

P A Erdman https://orcid.org/0000-0003-4626-2869

References

[1] Kosloff R 2013 Quantum thermodynamics: a dynamical viewpoint *Entropy* **15** 2100–28
[2] Kosloff R and Levy A 2014 Quantum heat engines and refrigerators: continuous devices *Annu. Rev. Phys. Chem.* **65** 365–93
[3] Benenti G, Casati G, Saito K and Whitney R S 2017 Fundamental aspects of steady-state conversion of heat to work at the nanoscale *Phys. Rep.* **694** 1–124
[4] Alicki R and Kosloff R 2018 Introduction to quantum thermodynamics: history and prospects *Thermodynamics in the Quantum Regime: Fundamental Aspects and New Directions* (Berlin: Springer) pp 1–33
[5] Buffoni L, Solfanelli A, Verrucchi P, Cuccoli A and Campisi M 2019 Quantum measurement cooling *Phys. Rev. Lett.* **122** 070603
[6] Pekola J P 2015 Towards quantum thermodynamics in electronic circuits *Nat. Phys.* **11** 118–23
[7] Goold J, Huber M, Riera A, del Rio L and Skrzypczyk P 2016 The role of quantum information in thermodynamics-a topical review *J. Phys. A: Math. Theor* **49** 143001
[8] Vinjanampathy S and Anders J 2016 Quantum thermodynamics *Contemp. Phys.* **57** 545–79
[9] Chen J 1994 The maximum power output and maximum efficiency of an irreversible Carnot heat engine *J. Phys. D: Appl. Phys.* **27** 1144
[10] Rezek Y and Kosloff R 2006 Irreversible performance of a quantum harmonic heat engine *New J. Phys.* **8** 83
[11] Scully M O, Chapin K R, Dorfman K E, Kim M B and Svidzinsky A 2011 Quantum heat engine power can be increased by noise-induced coherence *Proc. Natl Acad. Sci. USA* **108** 15097–100
[12] Abah O *et al* 2012 Single-ion heat engine at maximum power *Phys. Rev. Lett.* **109** 203006
[13] Correa L A, Palao J P, Adesso G and Alonso D 2013 Performance bound for quantum absorption refrigerators *Phys. Rev.* E **87** 042131
[14] Dorfman K E, Voronine D V, Mukamel S and Scully M O 2013 Photosynthetic reaction center as a quantum heat engine *Proc. Natl Acad. Sci. USA* **110** 2746–51
[15] Brunner N *et al* 2014 Entanglement enhances cooling in microscopic quantum refrigerators *Phys. Rev.* E **89** 032115
[16] Zhang K, Bariani F and Meystre P 2014 Quantum optomechanical heat engine *Phys. Rev. Lett.* **112** 150602
[17] Campisi M and Fazio R 2016 The power of a critical heat engine *Nat. Commun.* **7** 11895
[18] Roßnagel J *et al* 2016 A single-atom heat engine *Science* **352** 325–9
[19] Brandner K, Bauer M and Seifert U 2017 Universal coherence-induced power losses of quantum heat engines in linear response *Phys. Rev. Lett.* **119** 170602
[20] Watanabe G, Venkatesh B P, Talkner P and del Campo A 2017 Quantum performance of thermal machines over many cycles *Phys. Rev. Lett.* **118** 050601
[21] Josefsson M *et al* 2018 A quantum-dot heat engine operating close to the thermodynamic efficiency limits *Nat. Nanotechnol.* **13** 920–4
[22] Ronzani A *et al* 2018 Tunable photonic heat transport in a quantum heat valve *Nat. Phys.* **14** 991–5
[23] Prete D *et al* 2019 Thermoelectric conversion at 30 K in InAs/InP nanowire quantum dots *Nano Lett.* **19** 3033–9
[24] Esposito M, Kawai R, Lindenberg K and Van den Broeck C 2010 Efficiency at maximum power of low-dissipation carnot engines *Phys. Rev. Lett.* **105** 150603
[25] Wang J, He J and He X 2011 Performance analysis of a two-state quantum heat engine working with a single-mode radiation field in a cavity *Phys. Rev.* E **84** 041127
[26] Ludovico M F, Battista F, von Oppen F and Arrachea L 2016 Adiabatic response and quantum thermoelectrics for ac-driven quantum systems *Phys. Rev.* B **93** 075136
[27] Cavina V, Mari A and Giovannetti V 2017 Slow dynamics and thermodynamics of open quantum systems *Phys. Rev. Lett.* **119** 050601
[28] Abiuso P and Giovannetti V 2019 Control and non-Markovianity on a quantum thermal machine *Phys. Rev.* A **99** 052106
[29] Deng J, Wang Q-H, Liu Z, Hänggi P and Gong J 2013 Boosting work characteristics and overall heat-engine performance via shortcuts to adiabaticity: quantum and classical systems *Phys. Rev.* E **88** 062122
[30] Torrontegui E *et al* 2013 Ch 2-shortcuts to adiabaticity *Adv. At. Mol. Opt. Phys.* **62** 117–69
[31] del Campo A, Goold J and Paternostro M 2014 More bang for your buck: super-adiabatic quantum engines *Sci. Rep.* **4** 6208
[32] Çakmak B and Müstecaplıoğlu Ö E 2019 Spin quantum heat engines with shortcuts to adiabaticity *Phys. Rev.* E **99** 032108
[33] Rubin M H and Andresen B 1982 Optimal staging of endoreversible heat engines *J. Appl. Phys.* **53** 1
[34] Song H, Chen L and Sun F 2007 Endoreversible heat-engines for maximum power-output with fixed duration and radiative heat-transfer law *Appl. Energy* **84** 374–88
[35] Mukherjee V *et al* 2013 Speeding up and slowing down the relaxation of a qubit by optimal control *Phys. Rev.* A **88** 062326
[36] Bonnard B, Chyba M and Sugny D 2009 Time-minimal control of dissipative two-level quantum systems: the generic case *IEEE Trans. Autom. Control* **54** 2598–610
[37] Zhang T M, Wu R B, Zhang F H, Tarn T J and Long G L 2015 Minimum-time selective control of homonuclear spins *IEEE Trans. Control Syst. Technol* **23** 2018–25
[38] Roloff R, Wenin M and Pötz W 2009 Optimal control for open quantum systems: qubits and quantum gates *J. Comput. Theor. Nanosci.* **6** 1837–63
[39] Schulte-Herbrüggen T, Spörl A, Khaneja N and Glaser S J 2011 Optimal control for generating quantum gates in open dissipative systems *J. Phys. B: At. Mol. Opt. Phys.* **44** 154013
[40] Carlini A, Hosoya A, Koike T and Okudaira Y 2006 Time-optimal quantum evolution *Phys. Rev. Lett.* **96** 060503
[41] Sauer S, Gneiting C and Buchleitner A 2013 Optimal coherent control to counteract dissipation *Phys. Rev. Lett.* **111** 030405
[42] Campisi M, Pekola J and Fazio R 2015 Nonequilibrium fluctuations in quantum heat engines: theory, example, and possible solid state experiments *New J. Phys.* **17** 035012
[43] Cavina V, Mari A, Carlini A and Giovannetti V 2018 Variational approach to the optimal control of coherently driven, open quantum system dynamics *Phys. Rev.* A **98** 052125

[44] Suri N, Binder F C, Muralidharan B and Vinjanampathy S 2018 Speeding up thermalisation via open quantum system variational optimisation *Eur. Phys. J. Spec. Top.* **227** 203
[45] Cavina V, Mari A, Carlini A and Giovannetti V 2018 Optimal thermodynamic control in open quantum systems *Phys. Rev.* A **98** 012139
[46] Pekola J P, Karimi B, Thomas G and Averin D V 2019 Supremacy of incoherent sudden cycles *Phys. Rev.* B **100** 085405
[47] Menczel P, Pyhäranta T, Flindt C and Brandner K 2019 Two-stroke optimization scheme for mesoscopic refrigerators *Phys. Rev.* B **99** 224306
[48] Gorini V, Kossakowski A and Sudarshan E C G 1976 Completely positive dynamical semigroups of N-level systems *J. Math. Phys* **17** 821–5
[49] Lindblad G 1976 On the generators of quantum dynamical semigroups *Commun. Math. Phys.* **48** 119–30
[50] Feldmann T, Geva E, Kosloff R and Salamon P 1996 Heat engines in finite time governed by master equations *Am. J. Phys.* **64** 485–92
[51] Feldmann T and Kosloff R 2000 Performance of discrete heat engines and heat pumps in finite time *Phys. Rev.* E **61** 4774–90
[52] Cerino L, Puglisi A and Vulpiani A 2016 Linear and nonlinear thermodynamics of a kinetic heat engine with fast transformations *Phys. Rev.* E **93** 042116
[53] Curzon F L and Ahlborn B 1975 Efficiency of a Carnot engine at maximum power output *Am. J. Phys.* **43** 22–4
[54] Novikov I I 1958 Efficiency of an atomic power generating installation *J. Nucl. Energy* II **7** 125D128
[55] Chambadal P 1957 Les centrales nucleares *A. Colin* **4** 1
[56] Van den Broeck C 2005 Thermodynamic efficiency at maximum power *Phys. Rev. Lett.* **95** 190602
[57] Schmiedl T and Seifert U 2007 Efficiency at maximum power: an analytically solvable model for stochastic heat engines *Europhys. Lett.* **81** 20003
[58] Koski J V, Maisi V F, Pekola J P and Averin D V 2014 Experimental realization of a Szilard engine with a single electron *Proc. Natl Acad. Sci. USA* **111** 13786–9
[59] Maillet O *et al* 2019 Optimal probabilistic work extraction beyond the free energy difference with a single-electron device *Phys. Rev. Lett.* **122** 150604
[60] Breuer H P and Petruccione F 2002 *The Theory of Open Quantum Systems* (Oxford: Oxford University Press)
[61] Geva E and Kosloff R 1992 A quantum-mechanical heat engine operating in finite time. A model consisting of spin-1/2 systems as the working fluid *J. Chem. Phys.* **96** 3054–67
[62] Alicki R 1979 The quantum open system as a model of the heat engine *J. Phys. A: Math. Gen* **12** L103
[63] Senior J *et al* 2019 Heat rectification via a superconducting artificial atom arXiv:1908.05574
[64] Esposito M, Kawai R, Lindenberg K and Van den Broeck C 2010 Quantum-dot Carnot engine at maximum power *Phys. Rev.* E **81** 041106
[65] Esposito M, Lindenberg K and Van den Broeck C 2009 Thermoelectric efficiency at maximum power in a quantum dot *Europhys. Lett.* **85** 60010
[66] Dann R, Levy A and Kosloff R 2018 Time-dependent Markovian quantum master equation *Phys. Rev.* A **98** 052129
[67] Quan H T, Liu Y, Sun C P and Nori F 2007 Quantum thermodynamic cycles and quantum heat engines *Phys. Rev.* E **76** 031105
[68] Karimi B and Pekola J P 2016 Otto refrigerator based on a superconducting qubit: classical and quantum performance *Phys. Rev.* B **94** 184503
[69] Kosloff R and Rezek Y 2017 The quantum harmonic Otto cycle *Entropy* **19** 136
[70] Beenakker C W J 1991 Theory of Coulomb-blockade oscillations in the conductance of a quantum dot *Phys. Rev.* B **44** 1646
[71] Erdman P A *et al* 2017 Thermoelectric properties of an interacting quantum dot based heat engine *Phys. Rev.* B **95** 245432
[72] Wang J, Wu Z and He J 2012 Quantum Otto engine of a two-level atom with single-mode fields *Phys. Rev.* E **85** 041148
[73] Wegewijs M R and Nazarov Y V 1999 Resonant tunneling through linear arrays of quantum dots *Phys. Rev.* B **60** 14318–27
[74] Van Horne N *et al* 2018 Single atom energy-conversion device with a quantum load arXiv:1812.01303
[75] Chicone C 1999 *Ordinary Differential Equations with Applications* (New York: Springer)